Metal–Organic Frameworks Hot Paper

DOI: 10.1002/anie.201404265

Hydrogen Storage in a Potassium-Ion-Bound Metal–Organic Framework Incorporating Crown Ether Struts as Specific Cation Binding Sites**

*Dae-Woon Lim, Seung An Chyun, and Myunghyun Paik Suh**

Abstract: *To develop a metal–organic framework (MOF) for hydrogen storage, SNU-200 incorporating a 18-crown-6 ether moiety as a specific binding site for selected cations has been synthesized. SNU-200 binds K^+, NH_4^+, and methyl viologen (MV^{2+}) through single-crystal to single-crystal transformations. It exhibits characteristic gas-sorption properties depending on the bound cation. SNU-200 activated with supercritical CO_2 shows a higher isosteric heat (Q_{st}) of H_2 adsorption (7.70 kJ mol^{-1}) than other zinc-based MOFs. Among the cation inclusions, K^+ is the best for enhancing the isosteric heat of the H_2 adsorption (9.92 kJ mol^{-1}) as a result of the accessible open metal sites on the K^+ ion.*

Metal–organic frameworks (MOFs) have attracted considerable attention because of their various potential applications such as hydrogen storage,[1] carbon dioxide capture,[2] gas separation,[3] catalysis,[4] and fabrication of nanoparticles.[5] In particular, MOFs have been considered to be candidate materials for hydrogen storage, even though their practical applications are still limited as a result of unsolved problems, such as low gas-storage capacity at ambient temperature and low stability against water. To enhance H_2-storage capacities of MOFs at ambient temperature, the interaction energies between the frameworks and H_2 gas molecules should be increased. In general, MOFs interact with the guest molecules included in the pores through weak nonspecific interactions. To generate size-selective guest-binding properties or to induce strong interactions with the gas adsorbate, studies involving the control of pore aperture size and shape,[6] functionalization of the ligands,[7] and creation of vacant coordination sites on metal ions[8] have been conducted. The introduction of a guest-specific binding site or active domain has proven to be difficult, and there has been only one report to date, a pseudorotaxane-type MOF.[9] The MOF had organic struts attaching a 34- or 36-membered macrocyclic polyether pendant and it bound a paraquat dication (PQT^{2+}) guest by host–guest interactions. We previously revealed that the inclusion of specific guest molecules, 18-crown-6 and 15-crown-5, in the pores of a MOF provided an electrostatic field to enhance the binding energy of the H_2 gas molecules.[10] In addition, the impregnation of cations in a MOF has been shown to increase the gas-storage properties of the MOF.[2b] However, the selective inclusion of a desired cation in a MOF is still a challenging problem.

Herein, we report a MOF incorporating a 18-crown-6 (18Cr6) moiety as a framework component, $[Zn_5(\mu_3\text{-}OH)_2(TBADB\text{-}18Cr6)_2\cdot 4DMF]\cdot 13DMF\cdot 12H_2O$ (SNU-200; TBADB-18Cr6 = 4,4′,5,5′-terabenzoic acid dibenzo-18-crown-6, DMF = *N*,*N*-dimethylformamide), which provides specific guest binding sites for K^+, NH_4^+, and methyl viologen (MV^{2+}) cations. Upon binding of these cations, the MOF underwent a single-crystal to single-crystal transformation, and the X-ray crystal structures of the K^+ and NH_4^+ bound samples were able to be determined. The structure of the MV^{2+} bound MOF was characterized by "locate simulations" and powder X-ray diffraction (PXRD) patterns. SNU-200 and the cation bound samples, after activation with supercritical CO_2, adsorb N_2 and H_2 gases. The gas-sorption properties of the K^+ bound sample were compared with those of SNU-200′ (prime stands for sample activated by using supercritical CO_2) and the NH_4^+ bound MOF as well as the higher charged organic cation MV^{2+} bound MOF. Contrary to the previously reported MOFs,[11] the surface areas of the cation/counter-anion guest bound (K^+, NH_4^+, MV^{2+}/Cl^-, SCN^-) samples do not decrease compared to that of SNU-200′. SNU-200′ exhibits enhanced isosteric heat (Q_{st}) of H_2 adsorption compared to common Zn-MOFs.[12] Among K^+, NH_4^+, and MV^{2+} bound SNU-200′ analogues, the K^+ ion bound MOF shows the most highly enhanced isosteric heat (Q_{st}) of the H_2 adsorption.

To our knowledge, this is the first report on the gas-adsorption properties of a MOF incorporating a crown ether moiety as the framework component. Although there have been several reports for the synthesis of rotaxane-type MOFs,[13] they were incapable of adsorbing any gas molecules.

Colorless crystals of SNU-200 have been synthesized by heating a mixture of $Zn(NO_3)_2\cdot 6H_2O$ and H_4TBADB-18Cr6

[*] Dr. D.-W. Lim,[++] S. A. Chyun, Prof. M. P. Suh[+]
Department of Chemistry
Seoul National University
Seoul 151-747 (Republic of Korea)
E-mail: mpsuh@snu.ac.kr

[+] Current address: Department of Chemistry, Hanyang University
Seoul 133-791 (Republic of Korea)
E-mail: mpsuh@Hanyang.ac.kr

[++] Current address: Neutron Science Division, Korea Atomic Energy Research Institute (KAERI)
Daejeon, 305-353 (Republic of Korea)
E-mail: mpsuh@Hanyang.ac.kr

[**] This work was supported by National Research Foundation of Korea (NRF) Grant funded by the Korean Government (MEST) (No. 2005-0093842). We acknowledge the Pohang Accelerator Laboratory (PAL) for the use of the synchrotron 2D(SMC) beamline. D.-W.L. acknowledges support by Basic Science Research Fellowship from Seoul National University.

Supporting information for this article is available on the WWW under http://dx.doi.org/10.1002/anie.201404265.

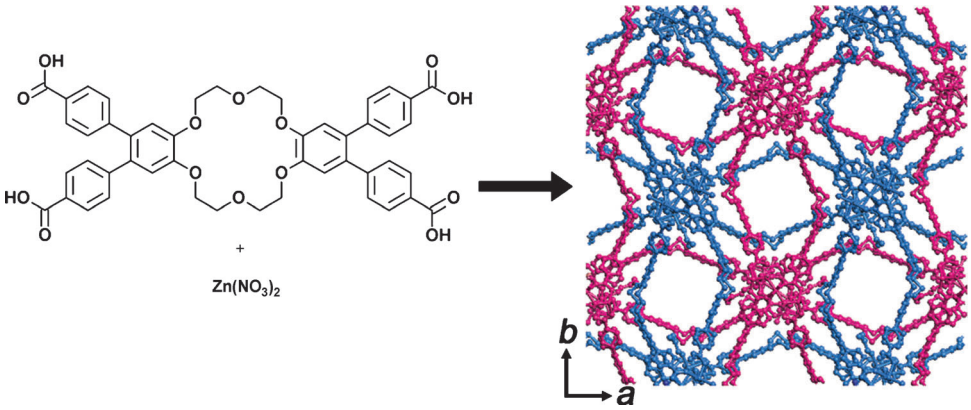

Figure 1. Synthesis and X-ray single crystal structure of doubly interpenetrated SNU-200. The networks are represented by two different colors. Hydrogen atoms are omitted for clarity.

in DMF/H_2O at 80 °C for 24 h. The X-ray crystal structure of SNU-200 exhibits a doubly interpenetrated 3D network generating 1D channels (8.4 Å) that extend along the *c*-axis (Figure 1). In a pore, two 18Cr6 face each other (Figure 2). There are three crystallographically independent Zn^{II} centers (Zn1, Zn2, and Zn3), and they are linked by an OH^- bridge as well as eight different carboxylates to form a Zn_5 cluster unit with the inversion center at Zn3 (Supporting Information, Figure S1). The Zn1 and Zn3 have an octahedral coordination geometry [∡O-Zn1-O, av. 89.63(4); ∡O-Zn3-O, av. 89.85(4)] and Zn2 has a tetrahedral geometry [∡O-Zn2-O, av. 109.66(6)]. The Zn1 atom is coordinated with two DMF solvent molecules. The solvent-accessible void volume estimated by PLATON is 39.2 % of the whole structure. Thermogravimetric analysis (TGA) data reveal a 41.0 % weight loss at 25–300 °C, which corresponds to the loss of all the coordinated DMF and guest solvent molecules (calcd 41.75 % for 13 DMF and 12 H_2O), and no chemical decomposition up to 350 °C (Supporting Information, Figure S2).

To see the specific cation binding in SNU-200, the crystals of SNU-200 were immersed in DMF solutions of K^+SCN^- (0.1 M), $NH_4^+Cl^-$ (0.01 M), and methyl viologen dichloride ($MV^{2+}2Cl^-$, 0.01 M), respectively, at room temperature for 3 days. K^+ and NH_4^+ ions have high binding constants for 18Cr6.[14] We expected that MV^{2+} would also interact with 18Cr6 strongly because it is electron deficient. KSCN was chosen as a K^+ source instead of KCl because of the easily identifiable SCN^- ion in the IR spectra, which would clearly indicate if it is coordinated at the metal ion or simply included in the pores of the MOFs. Furthermore, the solubility of KCl in DMF was too low (2–7 mmol L^{-1}) while NH_4Cl and $MV^{2+}Cl_2$ have solubilities high enough to satisfy the reaction conditions. After immersion, the extra salts included in the pores of the samples and adsorbed on the surface of the particles were removed by soaking the resulting crystals in fresh DMF for 24 h. During the cation inclusion, SNU-200 underwent single-crystal to single-crystal transformations, and the X-ray crystal structures of [K^+⊂SNU-200·SCN^-]·G and [NH_4^+⊂SNU-200]·Cl^-·G (G, guest solvents) could be determined.

The X-ray structure of [K^+⊂SNU-200·SCN^-]·G indicates that K^+ ion is located 0.0764(0.0061) Å above the mean plane made of the six oxygen atoms of 18Cr6 and it is coordinated with two water molecules at the axial sites (Figure 2, Figure S4).[15] In addition, one SCN^- ion replaces two DMF molecules and one carboxy oxygen atom coordinated at Zn1 of the pristine MOF, which alters the coordination geometry of Zn1 from octahedral to tetrahedral [∡N-Zn1-O, av. 111.46 (0.13); ∡O-Zn1-O, av. 107.66 (0.19)] (Figure S1). The SCN^- coordinates to Zn1 through a N atom as confirmed by a ν_{CN}

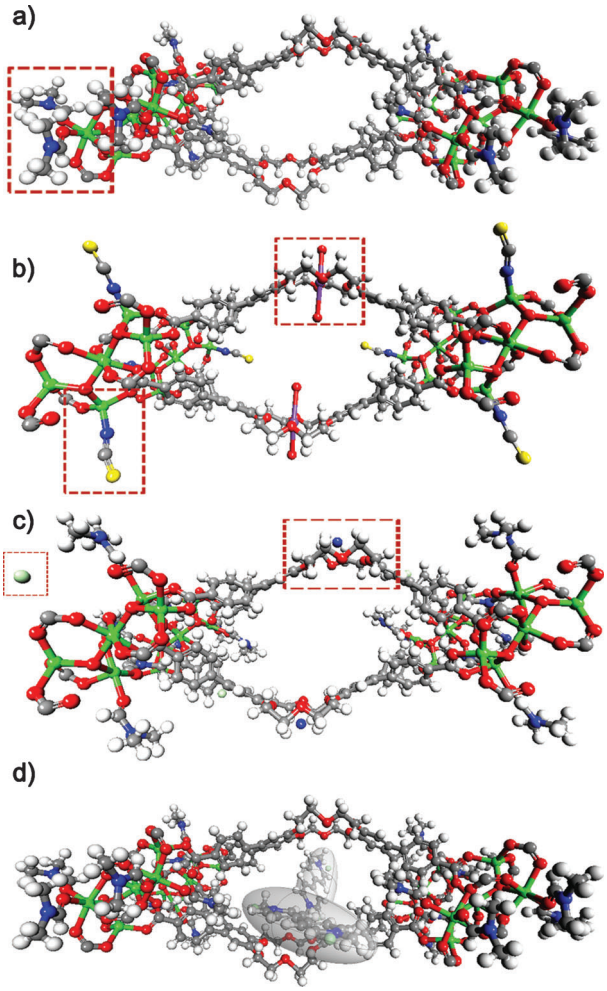

Figure 2. X-ray single-crystal structures[20] of as-synthesized a) SNU-200, b) [K^+⊂SNU-200·SCN^-]·G, and c) [NH_4^+⊂SNU-200]·Cl^-·G (G = guest). d) Structure of [MV^{2+}⊂SNU-200]·2 Cl^-·G obtained by "locate simulation", which is coincident with its PXRD data. Zn green, C black, H white, O red, N blue, Cl pale green and S yellow spheres. The binding sites of DMF molecules, cations, and their counteranions are highlighted by dashed red boxes. The gray ellipsoids indicate the location of MV^{2+} in the MOF.

band appearing at 2087 cm^{-1} in the IR spectrum (Figure S3). On activation of the framework with supercritical CO_2 fluid, two water molecules bound at each K^+ ion were removed as evidenced by the IR spectra (Figure S5).

In the X-ray structure of $[NH_4^+ \subset$SNU-200$]\cdot Cl^-\cdot$G, the coordination modes of the Zn ions in the Zn_5 cluster are the same as those of SNU-200, and each Zn1 still coordinates two DMF molecules. The NH_4^+ ion is positioned 1.577 (0.035) Å above the mean plane of 18Cr6. The NH_4^+ ion forms hydrogen bonds with the oxygen atoms of the crown ether with an average N–O distance of 2.949 (0.067) Å. The Cl^- counteranions are found in the channels. The elemental analysis data indicate that there are 1.09 NH_4^+ molecules per 18Cr6, implying that all the 18Cr6 moieties in the MOF bind NH_4^+ ions.

In $[MV^{2+} \subset$SNU-200$]\cdot 2\,Cl^-\cdot$G, SNU-200 also maintains single crystallinity after the immersion in a DMF solution of methyl viologen (ca. 0.01M). However, even with the synchrotron X-ray diffraction data collected at 100 K, the included methyl viologen species could not be located because of thermal disorder. Therefore, a "locate simulation" was performed using a sorption module of Materials Studio.[16] The Metropolis Monte Carlo method was chosen for the calculation of the global minimum locations. Universal force field (UFF) was selected for the energy calculation, and the charge equilibration (Q_{Eq}) method was used for the calculation of point atomic charges. The results indicate that MV^{2+} resides beside the 18-crown-6 moiety of SNU-200 (Figure 2), and a maximum of 4 methyl viologen molecules could be accommodated per unit cell, that is, one molecule per formula unit of SNU-200 (Supporting Information).

The powder X-ray diffraction (PXRD) patterns also indicate that the structure of SNU-200 is maintained even after the inclusion of KSCN, NH_4Cl, and methyl viologen dichloride inside or near the crown ether moiety (Figure S6). In particular, the PXRD pattern for the simulated structure of MV^{2+} loaded SNU-200 is coincident with the measured PXRD data of $[MV^{2+} \subset$SNU-200$]\cdot 2\,Cl^-\cdot$G, and the new peaks at the low-angle regions must correspond to the MV^{2+} guest molecules. After activation, however, the PXRD patterns of SNU-200′ and $[MV^{2+} \subset$SNU-200′$]\cdot 2\,Cl^-$ are slightly broadened together with the shift of the (101) peaks to a higher angle region (Figure S7), indicating shrinkage of the frameworks. Interestingly, the PXRD patterns for the activated samples of K^+ and NH_4^+ bound MOFs show better crystalline properties than the activated SNU-200 and $[MV^{2+} \subset$SNU-200$]\cdot 2\,Cl^-$. We assume that this occurs because the K^+ and NH_4^+ ions are bound within the 18Cr6 moieties, which make the framework more rigid upon activation compared to the other samples. All activated compounds are air sensitive, as evidenced by their PXRD patterns, which are highly broadened on exposure to air for 2 h (Figure S7).

To verify the porosity of the samples activated with supercritical CO_2 fluid, the adsorption–desorption isotherms of [SNU-200′], $[K^+ \subset$SNU-200′$\cdot SCN^-]$, $[NH_4^+ \subset$SNU-200′$]\cdot Cl^-$, and $[MV^{2+} \subset$SNU-200′$]\cdot 2\,Cl^-$ were measured for N_2 and H_2 gases at various temperatures (Table 1). The N_2 gas sorption isotherms of all samples show a type I curve, characteristic of the microporous materials (Figure S8). Contrary to other common MOFs,[11] the BET surface areas of the compounds including cations/counteranions are higher than that of SNU-200. This is because during the activation, the MOFs incorporating the cation bound 18Cr6 moieties together with the counteranion inclusions shrink less, than SNU-200.

Low pressure H_2 adsorption isotherms were measured at 77 K and 87 K under 1 atm (Figure 3). SNU-200′ uptakes H_2 gas up to 1.06 wt % at 77 K and 0.72 wt % at 87 K. It shows the

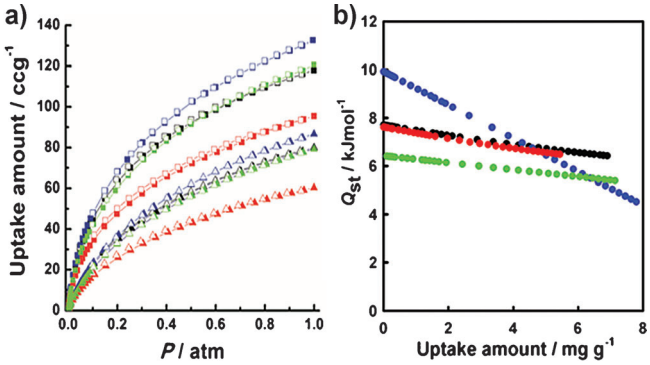

Figure 3. Gas-adsorption properties of SNU-200′ (black), $[K^+ \subset$SNU-200′$\cdot SCN^-]$ (navy), $[NH_4^+ \subset$SNU-200′$]\cdot Cl^-$ (green) and $[MV^{2+} \subset$SNU-200′$]\cdot 2\,Cl^-$ (red) a) H_2 gas sorption isotherms at 77 K (square) and 87 K (triangle). Filled shape: adsorption; open shape: desorption. b) Isosteric heat (Q_{st}) of H_2 adsorption.

enhanced isosteric heat (Q_{st}, 7.70 kJ mol^{-1}) of the H_2 adsorption compared to those of common Zn-MOFs (4.1–6.2 kJ mol^{-1}).[12] Interestingly, among the samples, $[K^+ \subset$SNU-200′$\cdot SCN^-]$ shows the highest H_2 uptake capacity, 1.19 wt % at 77 K and 0.78 wt % at 87 K, although its surface area is smaller than that of $[MV^{2+} \subset$SNU-200′$]\cdot 2\,Cl^-$. The zero-coverage isosteric heat of the H_2 adsorption in $[K^+ \subset$SNU-200′$\cdot SCN^-]$, which is estimated from the H_2 adsorption isotherms measured at 77 K and 87 K by using the virial equation, increases to 9.92 kJ mol^{-1} from 7.70 kJ mol^{-1} of SNU-200′ (Table 1, Figure 3). This enhance-

Table 1: H_2 sorption data of SNU-200′ and cation-bound SNU-200′ samples.

Compound	Ratio of cation/18Cr6	SA_{BET} [$m^2 g^{-1}$]	H_2 uptake [wt %]	Q_{st} of H_2 ads. [kJ mol^{-1}]
SNU-200′	N/A	736	1.06 (77 K)[d] 0.72 (87 K)[d] 0.26 (298 K)[e]	7.70
$[K^+ \subset$SNU-200′$\cdot SCN^-]$	0.92[a] (1.00)[c]	823	1.19 (77 K)[d] 0.78 (87 K)[d] 0.28 (298 K)[e]	9.92
$[NH_4^+ \subset$SNU-200′$]\cdot Cl^-$	1.09[b] (1.00)[c]	818	1.09 (77 K)[d] 0.71 (87 K)[d]	6.41
$[MV^{2+} \subset$SNU-200′$]\cdot 2Cl^-$	0.36[b] (0.50)[c]	935	0.86 (77 K)[d] 0.54 (87 K)[d]	7.62

[a] Based on the ICP data (found). [b] Based on the elemental analysis data. [c] Theoretical value ($mol_{cation}/mol_{ligand}$). [d] 1 atm. [e] 70 bar.

ment (by 2.22 kJ mol^{-1}) by the inclusion of the K^+ ion in the present MOF is much higher than the (by ca. 1.1 kJ mol^{-1}) previously reported values for the MOFs that included alkali-metal or alkali-earth-metal ions in the pores, which still coordinated the solvent molecules.[17] It is comparable to those of the Li^+ based MOFs.[18] The enhancement of the H_2 adsorption energy in [K^+⊂SNU-200′·SCN^-] is attributed to the K^+ ion having accessible open sites that were generated by the removal of the water molecules bound at K^+ ion upon activation of the sample. Although it was reported that the type of anions coordinated at the metal center of a MOF greatly affected the binding energy of the H_2 molecule,[1c] an anion effect on the Q_{st} values is not observed in the present case. At high pressure (70 bar) and 298 K, the amount (0.28 wt %) of H_2 adsorbed in [K^+⊂SNU-200′·SCN^-] is slightly higher than that (0.26 wt %) of SNU-200′ (Figure S10). The best MOF for hydrogen storage reported to date, [Ni(HTBC)(4,4′-bpy)], has an H_2 uptake capacity of 1.2 wt % at 298 K and 72 bar with the Q_{st} value of 8.8 kJ mol^{-1}.[19] In this respect, the Q_{st} value of the K^+ bound SNU-200 represents a significant finding. However, further work must be done to develop MOFs that have both high hydrogen uptake capacities at 298 K and high Q_{st} values.

To determine the position of an adsorbed H_2 molecule in [K^+⊂SNU-200·SCN^-], as-synthesized sample, we performed Grand Canonical Monte Carlo (GCMC) calculations by using a sorption module of Materials Studio (for detailed information, see Supporting Information).[16] The theoretical results indicate that a H_2 molecule is located above the K^+ ion in the crown ether moiety near the metal cluster, while it is positioned beside the metal clusters in the NH_4^+ and MV^{2+} bound MOFs (Figure S11).

In conclusion, a MOF incorporating a 18Cr6 crown ether moiety in the strut provides specific/selective binding sites for K^+, NH_4^+, and MV^{2+} ions. Pristine SNU-200′ has a higher isosteric heat of H_2 adsorption than the general Zn type MOFs. Among the cation/counteranion bound MOFs, the K^+ bound MOF exhibits the highest Q_{st} value of H_2 adsorption (9.92 kJ mol^{-1}) as a result of the accessible open metal sites on K^+, which are generated during activation. This work presents a significant step forward in tailoring MOFs to accommodate specific cations, which ultimately enhances the hydrogen-storage properties of this material.

Received: April 12, 2014
Published online: June 18, 2014

Keywords: cation inclusion · crown ethers · hydrogen storage · metal–organic frameworks · potassium ion

[1] a) M. P. Suh, H. J. Park, T. K. Prasad, D.-W. Lim, *Chem. Rev.* **2012**, *112*, 782–835; b) J. Sculley, D. Yuan, H.-C. Zhou, *Energy Environ. Sci.* **2011**, *4*, 2721–2735; c) K. Sumida, D. Stuck, L. Mino, J.-D. Chai, E. D. Bloch, O. Zavorotynska, L. J. Murray, M. Dinca, S. Chavan, S. Bordiga, M. Head-Gordon, J. R. Long, *J. Am. Chem. Soc.* **2013**, *135*, 1083–1091.

[2] a) H.-S. Choi, M. P. Suh, *Angew. Chem.* **2009**, *121*, 6997–7001; *Angew. Chem. Int. Ed.* **2009**, *48*, 6865–6869; b) H. J. Park, M. P. Suh, *Chem. Sci.* **2013**, *4*, 685–690; c) D. H. Hong, M. P. Suh, *Chem. Commun.* **2012**, *48*, 9168–9170; d) T. K. Kim, M. P. Suh, *Chem. Commun.* **2011**, *47*, 4258–4260.

[3] a) H. J. Park, Y. E. Cheon, M. P. Suh, *Chem. Eur. J.* **2010**, *16*, 11662–11669; b) H. J. Park, M. P. Suh, *Chem. Commun.* **2010**, *46*, 610–612.

[4] A. Corma, H. Garcia, F. X. L. Xamena, *Chem. Rev.* **2010**, *110*, 4606–4655.

[5] a) H. R. Moon, D.-W. Lim, M. P. Suh, *Chem. Soc. Rev.* **2013**, *42*, 1807–1824; b) D.-W. Lim, J. W. Yoon, K. Y. Ryu, M. P. Suh, *Angew. Chem.* **2012**, *124*, 9952–9955; *Angew. Chem. Int. Ed.* **2012**, *51*, 9814–9817; c) Y. E. Cheon, M. P. Suh, *Angew. Chem.* **2009**, *121*, 2943–2947; *Angew. Chem. Int. Ed.* **2009**, *48*, 2899–2903.

[6] a) J.-R. Li, R. J. Kuppler, H.-C. Zhou, *Chem. Soc. Rev.* **2009**, *38*, 1477–1504; b) L. Du, Z. Lu, K. Zheng, J. Wang, X. Zheng, Y. Pan, X. You, J. Bai, *J. Am. Chem. Soc.* **2013**, *135*, 562–565.

[7] a) J. L. C. Rowsell, O. M. Yaghi, *J. Am. Chem. Soc.* **2006**, *128*, 1304–1315; b) K. K. Tanabe, S. M. Cohen, *Chem. Soc. Rev.* **2011**, *40*, 498–519; c) J. Park, Z. U. Wang, L.-B. Sun, Y.-P. Chen, H.-C. Zhou, *J. Am. Chem. Soc.* **2012**, *134*, 20110–20116.

[8] Y.-G. Lee, H. R. Moon, Y. E. Cheon, M. P. Suh, *Angew. Chem.* **2008**, *120*, 7855–7859; *Angew. Chem. Int. Ed.* **2008**, *47*, 7741–7745.

[9] Q. Li, W. Zhang, O. Š. Miljanic, C.-H. Sue, Y.-L. Zhao, L. Liu, C. B. Knobler, J. F. Stoddart, O. M. Yaghi, *Science* **2009**, *325*, 855–859.

[10] H. J. Park, M. P. Suh, *Chem. Commun.* **2012**, *48*, 3400–3402.

[11] a) K. L. Mulfort, O. K. Farha, C. L. Stern, A. A. Sarjeant, J. T. Hupp, *J. Am. Chem. Soc.* **2009**, *131*, 3866–3868; b) K. L. Mulfort, J. T. Hupp, *Inorg. Chem.* **2008**, *47*, 7936–7938.

[12] a) B. Panella, M. Hirscher, *Adv. Mater.* **2005**, *17*, 538–541; b) J. Y. Lee, D. H. Olson, L. Pan, T. J. Emge, J. Li, *Adv. Funct. Mater.* **2007**, *17*, 1255–1262; c) W. Zhou, H. Wu, M. R. Hartman, T. Yildirim, *J. Phys. Chem. C* **2007**, *111*, 16131–16137; d) Z. Hulvey, D. A. Sava, J. Eckert, A. K. Cheetham, *Inorg. Chem.* **2011**, *50*, 403–405.

[13] a) Q. Li, C.-H. Sue, S. Basu, A. K. Shveyd, W. Zhang, G. Barin, L. Fang, A. A. Sarjeant, J. F. Stoddart, O. M. Yaghi, *Angew. Chem.* **2010**, *122*, 6903–6907; *Angew. Chem. Int. Ed.* **2010**, *49*, 6751–6755; b) A. Coskun, M. Hmadeh, G. Barin, F. Gándara, Q. Li, E. Choi, N. L. Strutt, D. B. Cordes, A. M. Z. Slawin, J. F. Stoddart, J.-P. Sauvage, O. M. Yaghi, *Angew. Chem.* **2012**, *124*, 2202–2205; *Angew. Chem. Int. Ed.* **2012**, *51*, 2160–2163; c) Y.-L. Zhao, L. Liu, W. Zhang, C.-H. Sue, Q. Li, O. Š. Miljanić, O. M. Yaghi, J. F. Stoddart, *Chem. Eur. J.* **2009**, *15*, 13356–13380.

[14] H. K. Frensdorff, *J. Am. Chem. Soc.* **1971**, *93*, 600–606.

[15] J. W. Steed, *Coord. Chem. Rev.* **2001**, *215*, 171–221.

[16] Materials Studio v5.5, Accelrys Inc., San Diego, CA, **2010**.

[17] F. Nouar, J. Eckert, J. F. Eubank, P. Forster, M. Eddaoudi, *J. Am. Chem. Soc.* **2009**, *131*, 2864–2870.

[18] a) S. Yang, X. Lin, A. J. Blake, G. S. Walker, P. Hubberstey, N. R. Champness, M. Schröder, *Nat. Chem.* **2009**, *1*, 487–493; b) S. Yang, G. S. B. Martin, J. J. Titman, A. J. Blake, D. R. Allan, N. R. Champness, M. Schröder, *Inorg. Chem.* **2011**, *50*, 9374–9384.

[19] Y. Li, L. Xie, Y. Liu, R. Yang, X. Li, *Inorg. Chem.* **2008**, *47*, 10372–10377.

[20] CCDC CCDC-920678 (SNU-200), 922626 ([K^+⊂SNU-200·SCN^-]·G), and 949494 ([NH_4^+⊂SNU-200]·Cl^-·G), contain the supplementary crystallographic data for this paper. These data can be obtained free of charge from The Cambridge Crystallographic Data Centre via www.ccdc.cam.ac.uk/data_request/cif.

